Partial polarization and electromagnetic spatial coherence of blackbody radiation emanating from an aperture

Kasimir Blomstedt
Department of Applied Physics, Aalto University, P.O. Box 13500, FI-00076 Aalto, Finland

Tero Setälä,* Jani Tervo, Jari Turunen, and Ari T. Friberg
Institute of Photonics, University of Eastern Finland, P.O. Box 111, FI-80101 Joensuu, Finland
(Received 29 May 2013; published 16 July 2013)

We consider, within the classical theory of electromagnetic coherence, the spectral coherence properties of a field emanating from an aperture in a blackbody cavity. Spatial coherence and polarization are assessed both in the aperture and in its far zone. We derive an expression for the full 3×3 cross-spectral density matrix of the field in the opening and discuss the validity of some related results given in the literature. The aperture field serves as a finite, planar secondary source whose transverse coherence length is found to be of the order of the wavelength and which is unpolarized in the three-dimensional sense. The far field is obtained by propagating each of the three source-field components separately, resulting in the evaluation of the far-field spatial coherence in any pair of directions, paraxial or nonparaxial. We show that in the paraxial case, the coherence properties coincide with those obtained for a planar, secondary source which is spatially δ-correlated and unpolarized. The results can find applications in the modeling of thermal sources and in the propagation of natural light fields.

DOI: 10.1103/PhysRevA.88.013824 PACS number(s): 42.25.Kb, 44.40.+a, 03.50.De, 42.25.Ja

I. INTRODUCTION

Blackbody radiation has had a pivotal role in the development of quantum mechanics and introduction of the concept of photons [1]. The coherence properties of blackbody radiation inside a cavity have been studied in the past within both the classical and the quantum theories, and the coherence matrices in the space-time domain [2–5] and in the space-frequency domain [6,7] are explicitly known (see also [8]). More recently, the spectral polarization properties of blackbody radiation emanating from an aperture in a cavity were analyzed and it was shown that the far field is unpolarized in every direction and obeys Lambert's law [9]. In addition, a few years ago the far-field spatial coherence matrix was derived in the paraxial region [10]. In both works the far field is obtained in terms of the two transverse electric-field components in the aperture, and explicit knowledge of the full 3×3 cross-spectral density matrix in the opening is not required.

In this paper, we construct the complete 3×3 electric cross-spectral density matrix of a field in an aperture of a cavity containing blackbody radiation. The aperture field differs from the field inside the cavity, as it only contains light exiting the cavity. The ensuing cross-spectral density matrix has not appeared in the literature before and we point out that some claims in previous works on the form of the aperture-field coherence matrix are inconsistent with our results. The field in the opening constitutes a finite, planar, secondary source whose statistical properties are quantified in terms of the electromagnetic degree of coherence [11–15] and the degree of polarization of three-dimensional (3D) fields [16–18]. We show that the spectral spatial coherence width of the source is of the order of the wavelength and the planar source is unpolarized in the 3D sense. These results are consistent with those found earlier for a blackbody field inside a cavity [19,20].

The far field is obtained in this work by propagating each of the three electric-field components separately into the far zone in terms of the Rayleigh diffraction formula. This approach leads to a correct cross-spectral density matrix [21] that is valid in any two directions, not necessarily confined to the paraxial regime. We show that in all directions the far-field spatial coherence extends over a very narrow angular separation, which is smaller the larger is the aperture. Under paraxial conditions the spatial coherence of the far field is shown to coincide with that produced by a spatially δ-correlated and two-dimensional (2D) unpolarized planar secondary source. Physical justification of the results is given.

The paper is organized as follows. In Sec. II the cross-spectral density matrix of the blackbody radiation in an aperture is derived and the partial polarization and partial electromagnetic coherence in the opening are quantified. Section III is devoted to the propagation of the aperture field into the far zone, while Sec. IV focuses on the characterization of the far-field coherence. Section V summarizes the main conclusions of this work.

II. CROSS-SPECTRAL DENSITY MATRIX AT THE APERTURE PLANE

Blackbody radiation inside a cavity can be viewed as a superposition of angularly uncorrelated and unpolarized plane waves whose intensities are the same and the propagation directions fill the whole 4π solid angle (see Fig. 1). This intuitive physical model corresponds to a statistically homogeneous and isotropic field whose cross-spectral density, in combination with Planck's law, is precisely that of blackbody radiation [2,19]. The radiation emanating from an opening in the wall of the cavity is composed of only those waves that propagate into a half-space. We set the aperture at the $z = 0$ plane and consider the field in the half-space $z > 0$.

*tero.setala@uef.fi

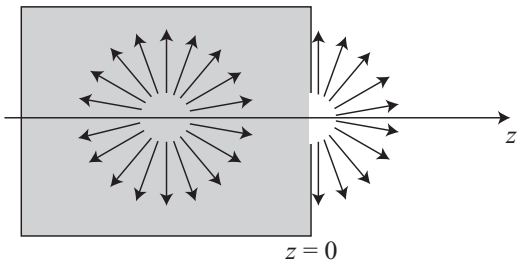

FIG. 1. Blackbody radiation inside a cavity can be regarded as a superposition of plane waves which is isotropic within the full 4π solid angle, whereas radiation emanating from the aperture is isotropic within the 2π solid angle. The aperture is at the $z = 0$ plane. The figure illustrates the situation in two dimensions.

The random electric field in the space-frequency domain produced by a superposition of plane waves propagating within the solid angle α is [19]

$$\mathbf{E}(\mathbf{r},\omega) = \int_\alpha \mathbf{A}(\hat{u},\omega)\exp(ik\hat{u}\cdot\mathbf{r})d\Omega, \tag{1}$$

where

$$\hat{u} = \sin\theta\cos\varphi\hat{u}_x + \sin\theta\sin\varphi\hat{u}_y + \cos\theta\hat{u}_z \tag{2}$$

is the unit vector that specifies the propagation direction of a plane wave in spherical polar coordinates (φ,θ) (see Fig. 2), with $\hat{u}_x$, $\hat{u}_y$, and $\hat{u}_z$ being the unit vectors along the Cartesian coordinate axes. The differential solid angle is given by $d\Omega = \sin\theta d\theta d\varphi$. In addition, $\mathbf{A}(\hat{u},\omega)$ is the random complex amplitude of the wave, ω is the angular frequency, and $k = \omega/c = 2\pi/\lambda$ is the wave number, with c being the speed of light in vacuum and λ the wavelength.

The vector amplitude can be decomposed as

$$\mathbf{A}(\hat{u},\omega) = A_s(\hat{u},\omega)\hat{s} + A_p(\hat{u},\omega)\hat{p}, \tag{3}$$

where $A_s(\hat{u},\omega)$ and $A_p(\hat{u},\omega)$ are the amplitudes of the s-polarized and p-polarized components, and $\hat{s} = \hat{u}_z \times \hat{u}/|\hat{u}_z \times \hat{u}|$ and $\hat{p} = \hat{s}\times\hat{u}$ are the related unit vectors (see Fig. 2). The electric-field vector is generally three-dimensional and we represent it by the column vector $\mathbf{E}(\mathbf{r},\omega) = [E_x(\mathbf{r},\omega), E_y(\mathbf{r},\omega), E_z(\mathbf{r},\omega)]^\mathsf{T}$, where T denotes transpose. For now we neglect the effect of the finite-sized aperture.

Equation (1) gives the realization of a random free field in the space-frequency domain. The cross-spectral density matrix

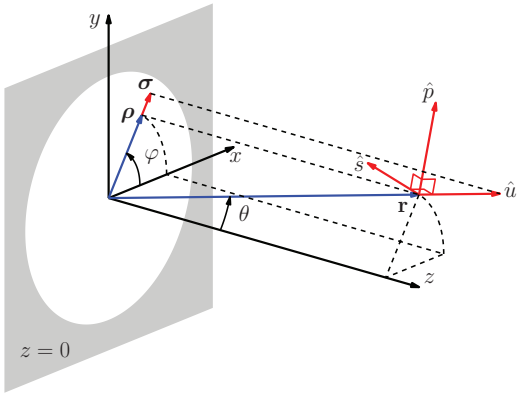

FIG. 2. (Color online) Illustration of notation.

can be written as

$$\begin{aligned}\mathbf{W}(\mathbf{r}_1,\mathbf{r}_2,\omega) &= \langle\mathbf{E}^*(\mathbf{r}_1,\omega)\mathbf{E}^\mathsf{T}(\mathbf{r}_2,\omega)\rangle \\ &= \int_\alpha\int_\alpha \langle\mathbf{A}^*(\hat{u}_1,\omega)\mathbf{A}^\mathsf{T}(\hat{u}_2,\omega)\rangle \\ &\quad\times\exp[-ik(\hat{u}_1\cdot\mathbf{r}_1 - \hat{u}_2\cdot\mathbf{r}_2)]d\Omega_1 d\Omega_2,\end{aligned} \tag{4}$$

where the asterisk and the angle brackets stand for the complex conjugate and ensemble average, respectively. Employing Eq. (3), the angular correlation matrix becomes

$$\begin{aligned}\langle\mathbf{A}^*(\hat{u}_1,\omega)\mathbf{A}^\mathsf{T}(\hat{u}_2,\omega)\rangle &= \langle A_s^*(\hat{u}_1,\omega)A_s(\hat{u}_2,\omega)\rangle\hat{s}_1\hat{s}_2^\mathsf{T} \\ &\quad+\langle A_s^*(\hat{u}_1,\omega)A_p(\hat{u}_2,\omega)\rangle\hat{s}_1\hat{p}_2^\mathsf{T} \\ &\quad+\langle A_p^*(\hat{u}_1,\omega)A_s(\hat{u}_2,\omega)\rangle\hat{p}_1\hat{s}_2^\mathsf{T} \\ &\quad+\langle A_p^*(\hat{u}_1,\omega)A_p(\hat{u}_2,\omega)\rangle\hat{p}_1\hat{p}_2^\mathsf{T}.\end{aligned} \tag{5}$$

For angularly uncorrelated and unpolarized plane waves whose intensities are the same we write

$$\begin{aligned}\langle A_s^*(\hat{u}_1,\omega)A_s(\hat{u}_2,\omega)\rangle &= \langle A_p^*(\hat{u}_1,\omega)A_p(\hat{u}_2,\omega)\rangle \\ &= a_0(\omega)\delta(\hat{u}_1 - \hat{u}_2),\end{aligned} \tag{6}$$

$$\langle A_s^*(\hat{u}_1,\omega)A_p(\hat{u}_2,\omega)\rangle = \langle A_p^*(\hat{u}_1,\omega)A_s(\hat{u}_2,\omega)\rangle = 0, \tag{7}$$

where $a_0(\omega)$ is a positive frequency-dependent constant and the directional Dirac δ function is given by $\delta(\hat{u}_1 - \hat{u}_2) = \delta(\varphi_2 - \varphi_1)\delta(\theta_2 - \theta_1)/|\sin(\theta_2)|$ [22]. The fact that the s-polarized and p-polarized components in each plane wave are mutually uncorrelated and have the same intensity ensures that the waves are 2D unpolarized, i.e., the degree of polarization of beam-like fields is 0 [23]. Inserting Eqs. (6) and (7) into Eq. (4) leads to

$$\mathbf{W}(\mathbf{r}_1,\mathbf{r}_2,\omega) = a_0(\omega)\int_\alpha(\mathbf{U}_3 - \hat{u}\hat{u}^\mathsf{T})\exp(ik\hat{u}\cdot\mathbf{R})d\Omega, \tag{8}$$

where $\mathbf{U}_3 = \hat{u}_x\hat{u}_x^\mathsf{T} + \hat{u}_y\hat{u}_y^\mathsf{T} + \hat{u}_z\hat{u}_z^\mathsf{T}$ is the 3×3 unit matrix and $\mathbf{R} = \mathbf{r}_2 - \mathbf{r}_1$. The above cross-spectral density matrix holds for a three-component field in 3D space and it is seen to be of statistically homogeneous form for any α. Introducing the aperture-plane vectors $\boldsymbol{\rho}$ and $\boldsymbol{\sigma}$ (see Fig. 2),

$$\boldsymbol{\rho} = x\hat{u}_x + y\hat{u}_y, \tag{9}$$

$$\boldsymbol{\sigma} = \sin\theta\cos\varphi\hat{u}_x + \sin\theta\sin\varphi\hat{u}_y, \tag{10}$$

we can write

$$\mathbf{r}_i = \boldsymbol{\rho}_i + z_i\hat{u}_z, \quad i\in(1,2), \tag{11}$$

$$\hat{u} = \boldsymbol{\sigma} + \cos\theta\hat{u}_z. \tag{12}$$

With this notation the cross-spectral density matrix in the $z = 0$ plane assumes the form

$$\mathbf{W}(\boldsymbol{\rho}_1,\boldsymbol{\rho}_2,\omega) = a_0(\omega)\int_\alpha(\mathbf{U}_3 - \hat{u}\hat{u}^\mathsf{T})\exp(ik\boldsymbol{\sigma}\cdot\boldsymbol{\rho})d\Omega, \tag{13}$$

where $\boldsymbol{\rho} = \boldsymbol{\rho}_2 - \boldsymbol{\rho}_1$. The angular integrations over the solid angle $\alpha = 2\pi$ (half-space $z > 0$) can be performed as outlined in Appendix A and the result is

$$\begin{aligned}\mathbf{W}(\boldsymbol{\rho}_1,\boldsymbol{\rho}_2,\omega) = 2\pi a_0(\omega)\Bigg\{&\left[j_0(k\rho) - \frac{j_1(k\rho)}{k\rho}\right]\mathbf{U}_3 \\ &+ j_2(k\rho)\hat{\rho}\hat{\rho}^\mathsf{T} - i\frac{J_2(k\rho)}{k\rho}\left(\hat{\rho}\hat{u}_z^\mathsf{T} + \hat{u}_z\hat{\rho}^\mathsf{T}\right)\Bigg\},\end{aligned} \tag{14}$$

where $\rho = |\boldsymbol{\rho}|$ and $\hat{\rho} = \boldsymbol{\rho}/\rho$. The functions $j_i(k\rho)$, with $i \in (0,1,2)$, are spherical Bessel functions of order i, and $J_2(k\rho)$ is the Bessel function of the first kind and order 2.

The matrix of Eq. (14) describes the spectral spatial coherence of an infinitely large planar secondary source formed by an isotropic (into the half-space $z > 0$) superposition of unpolarized and angularly uncorrelated plane waves. The finite size of the aperture, assumed to be circular and of radius ε, is incorporated by invoking Kirchoff's boundary conditions, which state that the field within the opening equals the incident (unperturbed) field and it is 0 elsewhere. Introducing the blocking function,

$$B(\boldsymbol{\rho}) = \begin{cases} 1 & \text{if} \quad \rho < \varepsilon, \\ 0 & \text{otherwise}, \end{cases} \tag{15}$$

the cross-spectral density matrix pertaining to the finite-sized, circular secondary source in the plane $z = 0$ takes the form

$$\mathbf{W}^{(0)}(\boldsymbol{\rho}_1,\boldsymbol{\rho}_2,\omega) = B(\boldsymbol{\rho}_1)B(\boldsymbol{\rho}_2)\mathbf{W}(\boldsymbol{\rho}_1,\boldsymbol{\rho}_2,\omega), \tag{16}$$

where $\mathbf{W}(\boldsymbol{\rho}_1,\boldsymbol{\rho}_2,\omega)$ is given by Eq. (14).

Up to now, we have not specified the spectral coefficient $a_0(\omega)$. The cross-spectral density matrix of blackbody radiation [6] is found if $4a_0(\omega)$ is chosen [19] to coincide with Planck's spectrum [24], i.e.,

$$4a_0(\omega) = \frac{2\hbar\omega^3}{\pi c^3}\frac{1}{\exp(\hbar\omega/k_B T) - 1}, \tag{17}$$

where $\hbar$ is the reduced Planck's constant, k_B the Boltzmann constant, and T the absolute temperature. The origin of the factor 4 is that the energy densities of the s-polarized and p-polarized electric fields are each $a_0(\omega)$, and the electric and magnetic fields contribute equally to the total energy density.

We note that some works state that the cross-spectral density matrix of the blackbody field in the aperture is one-half the matrix pertaining to the field inside the cavity [9,10]. This conclusion leads to a cross-spectral density matrix of the aperture field which otherwise equals Eq. (16) but the last term of Eq. (14) is absent. Whereas the energy is halved, physically it is understandable that the aperture correlation matrix can be different from the true blackbody correlation matrix across a plane since the plane waves propagating into the half-space $z < 0$ are missing. We soon see that the last term in Eq. (14) is necessary when all three electric field components are propagated separately, as it makes the far field obey the divergence (transversality) condition. The origin of the erroneous statements [9,10] appears to be that, in contrast to what is argued in [25], although a superposition of angularly uncorrelated scalar plane waves which is isotropic in the full 4π solid angle produces a sinc-form correlation function, a similar superposition within the 2π solid angle does not. In fact, it is likely that the coherence function related to the latter case cannot be expressed in a closed form except in the plane $z = 0$ and along the z axis. Incidentally, the situation resembles the decomposition of the point-dipole field into propagating and evanescent parts which have closed-form expressions only in the $z = 0$ plane and on the z axis [26]. Note also that the cross-spectral density matrix of Eq. (14) is of a statistically homogeneous form but it is not isotropic [27,28]. This is unlike

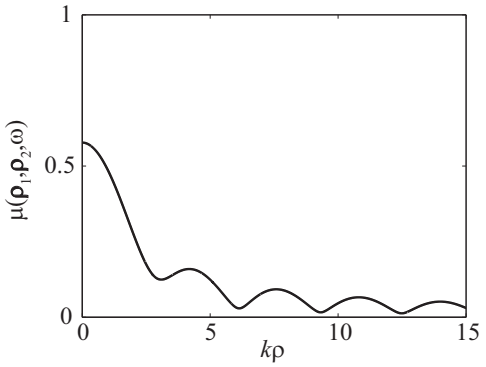

FIG. 3. Illustration of the electromagnetic degree of coherence as a function of $k\rho$, with $\rho = |\boldsymbol{\rho}_2 - \boldsymbol{\rho}_1|$, in the aperture of a blackbody cavity.

the blackbody radiation inside a cavity, which is known to be both homogeneous and isotropic [20].

The spatial coherence properties of the source can be quantified with the electromagnetic degree of coherence [11–15], $\mu(\mathbf{r}_1,\mathbf{r}_2,\omega)$, and the 3D degree of polarization [16–18], $P_3(\mathbf{r},\omega)$, defined, respectively, as

$$\mu^2(\mathbf{r}_1,\mathbf{r}_2,\omega) = \frac{\mathrm{tr}[\mathbf{W}^\dagger(\mathbf{r}_1,\mathbf{r}_2,\omega)\mathbf{W}(\mathbf{r}_1,\mathbf{r}_2,\omega)]}{\mathrm{tr}\mathbf{W}(\mathbf{r}_1,\mathbf{r}_1,\omega)\mathrm{tr}\mathbf{W}(\mathbf{r}_2,\mathbf{r}_2,\omega)}, \tag{18}$$

$$P_3^2(\mathbf{r},\omega) = \frac{3}{2}\left\{\frac{\mathrm{tr}\left[\boldsymbol{\Phi}_3^2(\mathbf{r},\omega)\right]}{\mathrm{tr}^2[\boldsymbol{\Phi}_3(\mathbf{r},\omega)]} - \frac{1}{3}\right\}, \tag{19}$$

where the dagger denotes the Hermitian adjoint, tr refers to the trace, and $\boldsymbol{\Phi}_3(\mathbf{r},\omega) = \mathbf{W}(\mathbf{r},\mathbf{r},\omega)$ is the 3×3 polarization matrix. Using Eq. (16) the degree of coherence in the aperture takes the form

$$\mu(\boldsymbol{\rho}_1,\boldsymbol{\rho}_2,\omega) = \frac{1}{\sqrt{3}}\left[j_0^2(k\rho) + \frac{1}{2}j_2^2(k\rho) + \frac{3}{2}\frac{J_2^2(k\rho)}{(k\rho)^2}\right]^{1/2}, \tag{20}$$

whose behavior as a function of $k\rho$ is shown in Fig. 3. The degree drops from $\mu(\boldsymbol{\rho},\boldsymbol{\rho},\omega) = 1/\sqrt{3}$, corresponding to an unpolarized 3D field [11], to a small number at approximately $k\rho = 6$. Therefore, we may say that the source correlations extend over the distance of the light's wavelength and the related (transverse) coherence length is $\rho_{\mathrm{coh}} \approx \lambda$. Approximately the same value for the coherence length is found for blackbody radiation inside the cavity, where the degree of coherence is otherwise the same as that in Eq. (20) but the last term is missing [20]. The degree of polarization defined in Eq. (19) is also readily calculated and is $P_3(\boldsymbol{\rho},\omega) = 0$, indicating explicitly that the planar source is 3D unpolarized, as is also the field inside the cavity [19].

III. PROPAGATION TO FAR ZONE

Once the realization of the electric field in the aperture plane is known there are at least two fundamentally different ways to propagate the field into the half-space $z > 0$ and the far zone. Since the two transverse aperture-field components uniquely determine the electric field throughout the domain $z > 0$, one can propagate the $E_x(\mathbf{r},\omega)$ and $E_y(\mathbf{r},\omega)$ components and compute $E_z(\mathbf{r},\omega)$ from the divergence condition [31]. This

approach amounts to the classic Luneburg equations [32] and it was used, e.g., in [9] to obtain the far field in spherical polar coordinates. Alternatively, one may calculate all three electric-field components directly on the basis that they all obey the Helmholtz equation [23]. This leads to a valid expression for the total electric field in the half-space $z > 0$ including the far zone, provided that the source field is correct (consistent with Maxwell's equations) [21]. We make use of the latter method in this work. From the realizations the cross-spectral density matrix is obtained by statistical averaging.

Mathematically the field realizations can be computed by means of Green's functions [33] or the angular spectrum decomposition [22,29]. The cross-spectral density matrices can also be propagated using the coherent modes [12] or elementary field representations [30]. Adopting the Green's function approach based on the Rayleigh diffraction formula for scalar waves [23], the far-zone electric-field components, $E_i^{(\infty)}(\mathbf{r},\omega)$, with $i \in (x,y,z)$, are written as

$$E_i^{(\infty)}(\mathbf{r},\omega) = \iint_{-\infty}^{\infty} E_i(\boldsymbol{\rho},\omega) G(\mathbf{r}-\boldsymbol{\rho},\omega) d^2\rho, \tag{21}$$

where the integration is over the $z = 0$ plane, and the Green's function is

$$G(\mathbf{r}-\boldsymbol{\rho},\omega) = -\frac{1}{2\pi}\frac{\partial}{\partial z}\left[\frac{\exp(ik|\mathbf{r}-\boldsymbol{\rho}|)}{|\mathbf{r}-\boldsymbol{\rho}|}\right]. \tag{22}$$

Far from the aperture we can approximate $|\mathbf{r}-\boldsymbol{\rho}| \approx r - \hat{u}\cdot\boldsymbol{\rho}$, and Eq. (22) assumes the form

$$G(\mathbf{r}-\boldsymbol{\rho},\omega) \approx -\frac{ik}{2\pi}\cos\theta\frac{\exp(ikr)}{r}\exp(-ik\hat{u}\cdot\boldsymbol{\rho}). \tag{23}$$

Using this in Eq. (21), the cross-spectral density matrix of the far field reads in the Cartesian coordinates as

$$\mathbf{W}^{(\infty)}(r_1\hat{u}_1, r_2\hat{u}_2, \omega) = (2\pi k)^2 \cos\theta_1 \cos\theta_2 \frac{\exp[ik(r_2 - r_1)]}{r_1 r_2} \times \mathbf{T}(\boldsymbol{\sigma}_1, \boldsymbol{\sigma}_2, \omega), \tag{24}$$

where

$$\mathbf{T}(\boldsymbol{\sigma}_1,\boldsymbol{\sigma}_2,\omega) = \frac{1}{(2\pi)^4}\iint_{-\infty}^{\infty}\iint_{-\infty}^{\infty}\mathbf{W}^{(0)}(\boldsymbol{\rho}_1,\boldsymbol{\rho}_2,\omega) \times \exp[-ik(\boldsymbol{\sigma}_2\cdot\boldsymbol{\rho}_2 - \boldsymbol{\sigma}_1\cdot\boldsymbol{\rho}_1)] d^2\rho_1 d^2\rho_2, \tag{25}$$

with $\mathbf{W}^{(0)}(\boldsymbol{\rho}_1,\boldsymbol{\rho}_2,\omega)$ given in Eq. (16). The matrix $\mathbf{T}(\boldsymbol{\sigma}_1,\boldsymbol{\sigma}_2,\omega)$ is the four-dimensional Fourier transform of the cross-spectral density matrix at the $z = 0$ plane. It can also be viewed as a matrix describing the correlation between the plane waves propagating in different directions and it could be constructed in terms of the angular-spectrum representation [29]. Assuming that the radius of the (circular) aperture is much larger than the wavelengths contained in the spectrum (which define the coherence length at each frequency) allows us to perform the integrations in Eq. (25) with the result (see Appendix B)

$$\mathbf{T}(\boldsymbol{\sigma}_1,\boldsymbol{\sigma}_2,\omega) = \frac{a_0(\omega)}{k^2}D(\sigma,\omega)(1-\bar{\sigma}^2)^{-1/2}\big[\mathbf{U}_3 - (1-\bar{\sigma}^2)\hat{u}_z\hat{u}_z^{\mathsf{T}} - \bar{\boldsymbol{\sigma}}\bar{\boldsymbol{\sigma}}^{\mathsf{T}} - (1-\bar{\sigma}^2)^{1/2}\big(\hat{u}_z\bar{\boldsymbol{\sigma}}^{\mathsf{T}} + \bar{\boldsymbol{\sigma}}\hat{u}_z^{\mathsf{T}}\big)\big], \tag{26}$$

with $\sigma = |\boldsymbol{\sigma}|$, $\boldsymbol{\sigma} = \boldsymbol{\sigma}_2 - \boldsymbol{\sigma}_1$ and $\bar{\sigma} = |\bar{\boldsymbol{\sigma}}|$, $\bar{\boldsymbol{\sigma}} = (\boldsymbol{\sigma}_1 + \boldsymbol{\sigma}_2)/2$. In addition,

$$D(\sigma,\omega) = \frac{\mathcal{A}_0}{2\pi^2}\frac{J_1(k\sigma\varepsilon)}{k\sigma\varepsilon}, \tag{27}$$

where $\mathcal{A}_0$ is the area of the circular aperture of radius ε. The cross-spectral density matrix in Eq. (24) is valid for any two directions $\hat{u}_1$ and $\hat{u}_2$, paraxial or nonparaxial. In the former case, apart from a multiplicative factor it reduces to the matrix presented earlier in the literature [10].

IV. FAR-ZONE COHERENCE

Inserting Eqs. (24), (26), and (27) into Eq. (18) gives

$$\mu(r_1\hat{u}_1, r_2\hat{u}_2, \omega) = \sqrt{2}\left|\frac{J_1(k\varepsilon\sigma)}{k\varepsilon\sigma}\right|\left[\frac{\cos\theta_1\cos\theta_2}{1-\bar{\sigma}^2}\right]^{1/2}, \tag{28}$$

for the degree of coherence of the far field. The validity of this expression is not restricted to the paraxial region. Note that the far-zone degree of coherence does not depend on the distances r_1 and r_2. The behavior of $\mu(r_1\hat{u}_1, r_2\hat{u}_2, \omega)$ as a function of θ_1 in the xz plane is illustrated for $\theta_2 = 0$ (paraxial geometry) and $\theta_2 = 3\pi/8$ (nonparaxial geometry) in Figs. 4(a) and 4(b), respectively. The dashed (blue) and solid (red) curves refer to $k\varepsilon = 100$ ($\varepsilon \approx 16\lambda$) and $k\varepsilon = 400$ ($\varepsilon \approx 64\lambda$), for which the assumption of the radius being large compared to the coherence length should hold. We observe that the spatial coherence extends over a larger angular separation in the nonparaxial direction than in the paraxial regime. In addition, the larger the aperture is, the smaller the angular separation over which the far field is spatially coherent. Note also that for small apertures the degree of coherence is asymmetric in the nonparaxial directions. In general, the angular separation is very small, of the order of milliradians.

It is insightful to compare, in the paraxial region, the far-field degree of coherence in Eq. (28) to that generated by a planar, circular secondary source which is spatially δ-correlated (zero coherence length) and unpolarized in the 2D sense. Such a source can be described by the cross-spectral density matrix,

$$\mathbf{W}^{(0)}(\boldsymbol{\rho}_1,\boldsymbol{\rho}_2,\omega) = S(\omega)B(\boldsymbol{\rho}_2)\mathbf{U}_2\delta(\boldsymbol{\rho}_2 - \boldsymbol{\rho}_1), \tag{29}$$

where $S(\omega)$ characterizes the spectral density, $B(\boldsymbol{\rho}_2)$ is the blocking function given in Eq. (15), and $\mathbf{U}_2 = \hat{u}_x\hat{u}_x^{\mathsf{T}} + \hat{u}_y\hat{u}_y^{\mathsf{T}}$. Substitution into Eq. (25) gives

$$\mathbf{T}(\boldsymbol{\sigma}_1,\boldsymbol{\sigma}_2,\omega) = \frac{S(\omega)D(\sigma,\omega)}{(2\pi)^2}\mathbf{U}_2, \tag{30}$$

which, when inserted into Eq. (24) and then into Eq. (18), results in

$$\mu(r_1\hat{u}_1, r_2\hat{u}_2, \omega) = \sqrt{2}\left|\frac{J_1(k\varepsilon\sigma)}{k\varepsilon\sigma}\right| \tag{31}$$

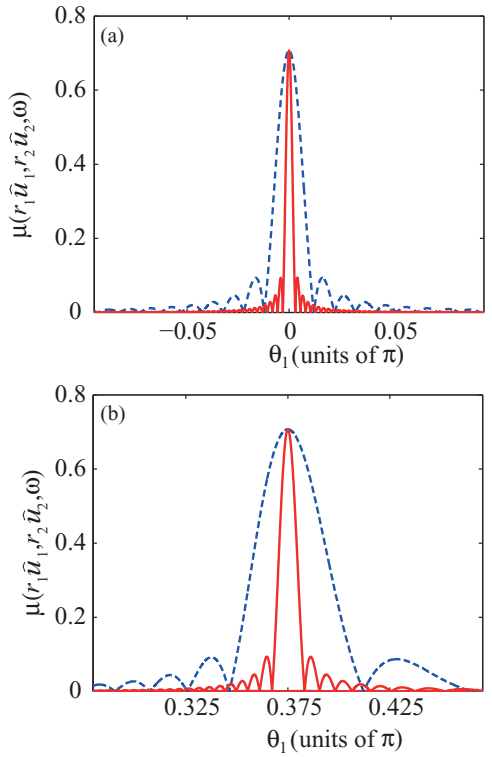

FIG. 4. (Color online) Illustration of the far-field electromagnetic degree of coherence as a function of θ_1 (in units of π) when (a) $\theta_2 = 0$ and (b) $\theta_2 = 3\pi/8$. In both cases $\varphi_1 = \varphi_2 = 0$, corresponding to the xz plane, while the dashed (blue) and solid (red) curves refer to $k\varepsilon = 100$ and $k\varepsilon = 400$, respectively. The peak values are $1/\sqrt{2}$.

for the far-field degree of coherence in the paraxial region. We note that the same formula is obtained with the far-zone form of the electromagnetic van Cittert–Zernike theorem [34]. The result in Eq. (31) is, to a good approximation, identical to Eq. (28) in the paraxial case ($\theta_1 \approx \theta_2 \approx 0$ and $\bar{\sigma} \approx 0$) for which the term in brackets is close to 1. The analysis therefore substantiates the intuitive conclusion that a planar, 2D unpolarized, δ-correlated secondary source is a highly accurate model for a planar, secondary thermal (blackbody) source when the field is considered in the paraxial regime. Physically this is evident already from Eq. (8), which, in the paraxial case, reduces to the low-spatial-frequency representation of Eq. (29).

The polarization matrix of the far field in any direction is obtained by setting $r_1\hat{u}_1 = r_2\hat{u}_2 = r\hat{u}$ in Eq. (24), leading to

$$\mathbf{\Phi}_3^{(\infty)}(r\hat{u},\omega) = \frac{a_0(\omega)\mathcal{A}_0\cos\theta}{r^2}(\mathbf{U}_3 - \hat{u}\hat{u}^{\mathsf{T}}). \tag{32}$$

Since $\mathbf{\Phi}_3^{(\infty)}(r\hat{u},\omega)\hat{u} = \hat{u}^{\mathsf{T}}\mathbf{\Phi}_3^{(\infty)}(r\hat{u},\omega) = 0$, the far field is transverse (planar) with respect to $\hat{u}$, as expected, and could be locally represented by a 2×2 polarization matrix and characterized by the degree of polarization of beam-like fields [23]. We can equally well describe the degree of polarization in terms of a 3D formalism. Substituting Eq. (32) into Eq. (19) implies that $P_3(r\hat{u},\omega) = 1/2$ for all directions and hence the field is unpolarized in the 2D sense [18]. This is in agreement with [9] and [10]. Note that the equal-point and the equal-direction far-field degrees of coherence take on the value $\mu(r\hat{u},r\hat{u},\omega) = \mu(r_1\hat{u},r_2\hat{u},\omega) = 1/\sqrt{2}$, corresponding to a 2D unpolarized plane wave [11]. The equal-direction degree of coherence is not unity since the fields at two points in a fixed direction are not completely correlated.

The radiant intensity (power per solid angle) in the direction $\hat{u}$ is also readily obtained as

$$\begin{aligned} J(\hat{u},\omega) &= \lim_{r\to\infty}\left\{r^2\mathrm{tr}\left[\mathbf{\Phi}_3^{(\infty)}(r\hat{u},\omega)\right]\right\} \\ &= 2a_0(\omega)\mathcal{A}_0\cos\theta \\ &= \frac{1}{2}\frac{2\hbar\omega^3}{\pi c^3}\frac{\mathcal{A}_0\cos\theta}{\exp(\hbar\omega/k_BT)-1}, \end{aligned} \tag{33}$$

where Planck's law of Eq. (17) is inserted in the last equality. The factor $1/2$ comes from the fact that only the waves propagating into the half-space $z > 0$ are included. The result in Eq. (33) shows that the aperture field is a Lambertian source consistent with [9]. The aperture-field coherence of planar scalar-wave Lambertian sources has been discussed, e.g., in [7] and [35].

V. CONCLUSIONS

In this work we have derived the full 3×3 cross-spectral density matrix for a field in the aperture of a blackbody cavity. Unlike results reported in some works in the literature, this aperture-field matrix differs in form from the cross-spectral density matrix of blackbody radiation within the cavity. The spectral coherence length in the opening was found to be of the order of the wavelength, and the field was shown to be unpolarized in the 3D sense. Consistent with previous results, the far field emitted from the aperture was demonstrated to be 2D unpolarized in every direction and to obey Lambert's law. We have derived the far-field electromagnetic degree of coherence, which holds in both the paraxial and the nonparaxial situations, and demonstrated that the spatial coherence extends over very narrow angular separations. We have compared the spatial coherence in the paraxial case to that generated by a planar, secondary, spatially δ-correlated and 2D unpolarized source. To a good accuracy, the two sources produce the same far-field coherence, indicating that a spatially δ-correlated, unpolarized secondary source is a good model for a thermally emitting radiator. The findings of this work add to the existing results on blackbody radiation, which possesses a fundamental place in the development of quantum physics. The results of this work can have applications in the modeling of thermal sources and in the propagation of natural light fields.

ACKNOWLEDGMENT

This work was supported by Dean's special funding for coherence research at the University of Eastern Finland, Joensuu (Project No. 930350).

APPENDIX A: ANGULAR INTEGRATIONS IN EQ. (13)

Making use of Eq. (12) we can rewrite Eq. (13) as

$$\begin{aligned} \mathbf{W}(\boldsymbol{\rho}_1,\boldsymbol{\rho}_2,\omega) = a_0(\omega)\int_\alpha \big[&\mathbf{U}_3 - \boldsymbol{\sigma}\boldsymbol{\sigma}^{\mathsf{T}} - \cos^2\theta\,\hat{u}_z\hat{u}_z^{\mathsf{T}} \\ &- \cos\theta\left(\boldsymbol{\sigma}\hat{u}_z^{\mathsf{T}} + \hat{u}_z\boldsymbol{\sigma}^{\mathsf{T}}\right)\big]\exp(ik\boldsymbol{\sigma}\cdot\boldsymbol{\rho})d\Omega, \end{aligned} \tag{A1}$$

where the angular integrations over the half-space solid angle of $\alpha = 2\pi$ can be carried out. For the first term one finds

$$\int_{2\pi} \exp(ik\boldsymbol{\sigma}\cdot\boldsymbol{\rho})d\Omega = 2\pi j_0(k\rho), \tag{A2}$$

while the second term is developed as

$$\begin{aligned}\int_{2\pi} \boldsymbol{\sigma}\boldsymbol{\sigma}^{\mathsf{T}} \exp(ik\boldsymbol{\sigma}\cdot\boldsymbol{\rho})d\Omega &= -\frac{1}{k^2}\nabla_{\boldsymbol{\rho}}\nabla_{\boldsymbol{\rho}}^{\mathsf{T}}\int_{2\pi}\exp(ik\boldsymbol{\sigma}\cdot\boldsymbol{\rho})d\Omega \\ &= 2\pi\left[\frac{j_1(k\rho)}{k\rho}\mathbf{U}_2 - j_2(k\rho)\hat{\rho}\hat{\rho}^{\mathsf{T}}\right],\end{aligned} \tag{A3}$$

where $\nabla_{\boldsymbol{\rho}}$ denotes the derivative with respect to $\boldsymbol{\rho}$ and $\mathbf{U}_2 = \hat{u}_x\hat{u}_x^{\mathsf{T}} + \hat{u}_y\hat{u}_y^{\mathsf{T}}$. In the derivation of Eq. (A3) the result in Eq. (A2) and the facts that $\nabla_{\boldsymbol{\rho}}\rho = \hat{\rho}$ and $\nabla_{\boldsymbol{\rho}}\boldsymbol{\rho} = \mathbf{U}_2$ were used. For the third term we employ

$$\int_{2\pi}\exp(ik\boldsymbol{\sigma}\cdot\boldsymbol{\rho})\cos^2\theta d\Omega = 2\pi\frac{j_1(k\rho)}{k\rho}. \tag{A4}$$

The last term is integrated using the explicit form of $\boldsymbol{\sigma}$ given in Eq. (10) and the formula

$$\begin{aligned}&\int_{2\pi}\exp(ik\boldsymbol{\sigma}\cdot\boldsymbol{\rho})\cos\theta\sin\theta\begin{Bmatrix}\cos\varphi\\ \sin\varphi\end{Bmatrix}d\Omega \\ &\quad = 2i\pi\frac{J_2(k\rho)}{k\rho}\begin{Bmatrix}\hat{\rho}_x\\ \hat{\rho}_y\end{Bmatrix},\end{aligned} \tag{A5}$$

where $\hat{\rho}_i$, with $i \in (x,y)$, are the components of $\hat{\rho}$. Collecting the above integrals leads to Eq. (14).

APPENDIX B: INTEGRATIONS IN EQ. (25)

Introducing the integration variables $\boldsymbol{\rho} = \boldsymbol{\rho}_2 - \boldsymbol{\rho}_1$ and $\bar{\boldsymbol{\rho}} = (\boldsymbol{\rho}_1 + \boldsymbol{\rho}_2)/2$, Eq. (25) becomes

$$\begin{aligned}\mathbf{T}(\boldsymbol{\sigma}_1,\boldsymbol{\sigma}_2,\omega) = \frac{a_0(\omega)}{(2\pi)^3}&\iint_{-\infty}^{\infty}\exp(-ik\boldsymbol{\sigma}\cdot\bar{\boldsymbol{\rho}}) \\ &\times\iint_{-\infty}^{\infty}B\left(\bar{\boldsymbol{\rho}}+\frac{\boldsymbol{\rho}}{2}\right)B\left(\bar{\boldsymbol{\rho}}-\frac{\boldsymbol{\rho}}{2}\right) \\ &\times\left\{\left[j_0(k\rho)-\frac{j_1(k\rho)}{k\rho}\right]\mathbf{U}_3 + j_2(k\rho)\hat{\rho}\hat{\rho}^{\mathsf{T}}\right. \\ &\left.-i\frac{J_2(k\rho)}{k\rho}\left(\hat{\rho}\hat{u}_z^{\mathsf{T}}+\hat{u}_z\hat{\rho}^{\mathsf{T}}\right)\right\} \\ &\times\exp(-ik\bar{\boldsymbol{\sigma}}\cdot\boldsymbol{\rho})d^2\rho d^2\bar{\rho},\end{aligned} \tag{B1}$$

where $\boldsymbol{\sigma} = \boldsymbol{\sigma}_2 - \boldsymbol{\sigma}_1$ and $\bar{\boldsymbol{\sigma}} = (\boldsymbol{\sigma}_1 + \boldsymbol{\sigma}_2)/2$ as before. We next use the fact that the coherence length of the source (at frequency ω) is of the order of the wavelength and hence much less than the diameter of the aperture. In other words, the width of the term in the curly brackets in the latter integral is much less than the aperture dimension. This allows us, to a good approximation, to remove the blocking functions from the latter integral. We note that $B^2(\bar{\boldsymbol{\rho}},\omega) = B(\bar{\boldsymbol{\rho}},\omega)$ and define

$$D(\boldsymbol{\sigma},\omega) = \frac{1}{(2\pi)^2}\iint_{-\infty}^{\infty}B(\bar{\boldsymbol{\rho}})\exp(-ik\boldsymbol{\sigma}\cdot\bar{\boldsymbol{\rho}})d^2\bar{\rho}, \tag{B2}$$

which is the 2D spatial Fourier transform of the blocking function. For a circular aperture it becomes $D(\boldsymbol{\sigma},\omega) = D(\sigma,\omega)$ and equals Eq. (27). Noting also that $\hat{\rho} = \boldsymbol{\rho}/\rho$, changing the variables as $\mathbf{R} = k\boldsymbol{\rho}$ and using the fact that $\mathbf{R}\exp(-i\bar{\boldsymbol{\sigma}}\cdot\mathbf{R}) = i\nabla_{\bar{\boldsymbol{\sigma}}}\exp(-i\bar{\boldsymbol{\sigma}}\cdot\mathbf{R})$, where $\nabla_{\bar{\boldsymbol{\sigma}}}$ denotes the derivative with respect to $\bar{\boldsymbol{\sigma}}$, enables us to write

$$\begin{aligned}\mathbf{T}(\boldsymbol{\sigma}_1,\boldsymbol{\sigma}_2,\omega) = \frac{a_0(\omega)D(\sigma,\omega)}{2\pi k^2}&\iint_{-\infty}^{\infty}\left\{\left[j_0(R)-\frac{j_1(R)}{R}\right]\mathbf{U}_3\right. \\ &-\frac{j_2(R)}{R^2}\nabla_{\bar{\boldsymbol{\sigma}}}\nabla_{\bar{\boldsymbol{\sigma}}}^{\mathsf{T}} + \frac{J_2(R)}{R^2}\left(\nabla_{\bar{\boldsymbol{\sigma}}}\hat{u}_z^{\mathsf{T}} + \hat{u}_z\nabla_{\bar{\boldsymbol{\sigma}}}^{\mathsf{T}}\right)\Big\} \\ &\times\exp(-i\bar{\boldsymbol{\sigma}}\cdot\mathbf{R})d^2R,\end{aligned} \tag{B3}$$

where $R = |\mathbf{R}|$. The integrations can readily be performed by taking the derivatives out of the integral and using circular cylindrical coordinates. The angular integrations are done with the help of the formula

$$\int_0^{2\pi}\exp[-i\bar{\sigma}R\cos(\beta-\beta')]d\beta = 2\pi J_0(\bar{\sigma}R), \tag{B4}$$

where β and β' are the angles that the vectors $\mathbf{R}$ and $\bar{\boldsymbol{\sigma}}$ make with respect to the x axis, and $J_0(\bar{\sigma}R)$ is the Bessel function of the first kind and order 0. For radial integrations we use the results

$$\int_0^{\infty}Rj_0(R)J_0(\bar{\sigma}R)dR = (1-\bar{\sigma}^2)^{-1/2}, \tag{B5}$$

$$\int_0^{\infty}j_1(R)J_0(\bar{\sigma}R)dR = (1-\bar{\sigma}^2)^{1/2}, \tag{B6}$$

$$\int_0^{\infty}R^{-1}j_2(R)J_0(\bar{\sigma}R)dR = \frac{1}{3}(1-\bar{\sigma}^2)^{3/2}, \tag{B7}$$

$$\int_0^{\infty}R^{-1}J_2(R)J_0(\bar{\sigma}R)dR = \frac{1}{2}(1-\bar{\sigma}^2). \tag{B8}$$

These equations are found by expressing the spherical Bessel functions in terms of the ordinary Bessel functions with the help of the relation $j_i(x) = \sqrt{\pi/2x}J_{i+1/2}(x)$, and making use of Eqs. (A2), (A4) and (A5) of [9]. After the integrations Eq. (B3) takes on the form

$$\begin{aligned}\mathbf{T}(\boldsymbol{\sigma}_1,\boldsymbol{\sigma}_2,\omega) = \frac{a_0(\omega)D(\sigma,\omega)}{k^2}&\left[\frac{\bar{\sigma}^2}{(1-\bar{\sigma}^2)^{1/2}}\mathbf{U}_3\right. \\ &+\frac{1}{3}\nabla_{\bar{\boldsymbol{\sigma}}}\nabla_{\bar{\boldsymbol{\sigma}}}^{\mathsf{T}}(1-\bar{\sigma}^2)^{3/2} \\ &\left.+\frac{1}{2}\left(\nabla_{\bar{\boldsymbol{\sigma}}}\hat{u}_z+\hat{u}_z\nabla_{\bar{\boldsymbol{\sigma}}}^{\mathsf{T}}\right)(1-\bar{\sigma}^2)\right].\end{aligned} \tag{B9}$$

The derivations can be done with the help of the identities $\nabla_{\bar{\sigma}}\bar{\sigma} = \bar{\boldsymbol{\sigma}}/\bar{\sigma}$ and $\nabla_{\bar{\boldsymbol{\sigma}}}\bar{\boldsymbol{\sigma}} = \mathbf{U}_2$, leading straightforwardly to Eq. (26).

[1] M. Planck, Ann. Phys. **4**, 553 (1901).
[2] R. C. Bourret, Nuovo Cimento **18**, 347 (1960).
[3] Y. Kano and E. Wolf, Proc. Phys. Soc. **80**, 1273 (1962).
[4] C. L. Mehta and E. Wolf, Phys. Rev. **134**, A1143 (1964).
[5] C. L. Mehta and E. Wolf, Phys. Rev. **134**, A1149 (1964).
[6] C. L. Mehta and E. Wolf, Phys. Rev. **161**, 1328 (1967).

[7] W. H. Carter and E. Wolf, J. Opt. Soc. Am. **65**, 1067 (1975).
[8] G. S. Agarwal, Phys. Rev. A **11**, 230 (1975).
[9] D. F. V. James, Opt. Commun. **109**, 209 (1994).
[10] M. Lahiri and E. Wolf, Opt. Commun. **281**, 3241 (2008).
[11] J. Tervo, T. Setälä, and A. T. Friberg, Opt. Express. **11**, 1137 (2003).
[12] J. Tervo, T. Setälä, and A. T. Friberg, J. Opt. Soc. Am. A **21**, 2205 (2004).
[13] T. Setälä, J. Tervo, and A. T. Friberg, Opt. Lett. **29**, 328 (2004).
[14] T. Setälä, J. Tervo, and A. T. Friberg, Opt. Lett. **31**, 2669 (2006).
[15] J. Tervo, T. Setälä, and A. T. Friberg, Opt. Lett. **37**, 151 (2012).
[16] T. Setälä, M. Kaivola, and A. T. Friberg, Phys. Rev. Lett. **88**, 123902 (2002).
[17] T. Setälä, A. Shevchenko, M. Kaivola, and A. T. Friberg, Phys. Rev. E **66**, 016615 (2002).
[18] T. Setälä, K. Lindfors, and A. T. Friberg, Opt. Lett. **34**, 3394 (2009).
[19] T. Setälä, M. Kaivola, and A. T. Friberg, Opt. Lett. **28**, 1069 (2003).
[20] T. Setälä, J. Lindberg, K. Blomstedt, J. Tervo, and A. T. Friberg, Phys. Rev. E **71**, 036618 (2005).
[21] O. Korotkova and E. Wolf, J. Opt. Soc. Am. A **21**, 2382 (2004).
[22] M. Nieto-Vesperinas, in *Scattering and Diffraction in Physical Optics* (Wiley, New York, 1991), p. 154.
[23] L. Mandel and E. Wolf, *Optical Coherence and Quantum Optics* (Cambridge University Press, Cambridge, UK, 1995).
[24] B. E. A. Saleh and M. C. Teich, in *Fundamentals of Photonics*, 2nd ed. (Wiley, Hoboken, NJ, 2007), p. 520.
[25] F. Gori, D. Ambrosini, and V. Bagini, Opt. Commun. **107**, 331 (1994).
[26] T. Setälä, M. Kaivola, and A. T. Friberg, Phys. Rev. E **59**, 1200 (1999).
[27] T. Setälä, K. Blomstedt, M. Kaivola, and A. T. Friberg, Phys. Rev. E **67**, 026613 (2003).
[28] G. K. Batchelor, in *The Theory of Homogeneous Turbulence* (Cambridge University Press, Cambridge, UK, 1970), Secs. 3.3 and 3.4.
[29] J. Tervo and J. Turunen, Opt. Commun. **209**, 7 (2002).
[30] J. Tervo, J. Turunen, P. Vahimaa, and F. Wyrowski, J. Opt. Soc. Am. A **27**, 2004 (2010).
[31] J. D. Jackson, *Classical Electrodynamics*, 3rd ed. (Wiley, New York, 1999).
[32] R. K. Luneburg, *Mathematical Theory of Optics* (University of California Press, Berkeley, 1964).
[33] C.-T. Tai, *Dyadic Green's Functions in Electromagnetic Theory* (Intext, Scranton, PA, 1971).
[34] J. Tervo, T. Setälä, J. Turunen, and A. T. Friberg, Opt. Lett. **38**, 2301 (2013).
[35] A. Starikov and A. T. Friberg, Appl. Opt. **23**, 4261 (1984).